EXPERIMENTAL PUSHOVER TESTING OF A FULL-SCALE UNREINFORCED CLAY BRICK MASONRY BUILDING

L.S. Hogan, K.Q. Walsh, J.M. Ingham, and D. Dizhur

Department of Civil and Environmental Engineering, University of Auckland, New Zealand.

ABSTRACT: Due to the large number of existing unreinforced masonry (URM) buildings in New Zealand, and the significant seismic hazard that this building stock represents, a significant effort has been recently made to quantify the seismic behaviour of such buildings in order to provide assessment guidance to practicing structural engineers and to help inform seismic retrofit solutions. The current assessment guidelines have yet to be benchmarked with the results of a large scale test of typical URM buildings. In response, field testing was performed on a decommissioned vintage URM building to investigate the in-situ behaviour of URM piers and compare actual behaviour to that predicted by existing assessment frameworks. The tested building was a prototypical, three-storey, 1930s fired clay brick URM building located in Auckland, New Zealand. A pushover test was performed by applying a load to the roof level of the building with a 22 tonne excavator, resulting in the formation of a pier rocking mechanism consistent with the predicted modes determined using current assessment guidelines for URM piers.

1 INTRODUCTION

Unreinforced masonry (URM) buildings represent one of the most seismically vulnerable building types, and their prevalence in high seismic areas has resulted in a significant amount of research being undertaken to provide techniques for the performance assessment of these buildings. While this research provided valuable inputs for the development of these assessment tools, the tests typically represented building components with idealised boundary conditions (Knox 2012). There has been little testing of URM buildings at large scale to evaluate the existing assessment tools. In response, monotonic pushover testing was performed on a URM building scheduled for demolition in Auckland, New Zealand. One elevation of the tested building was subjected to a point load generated by a 22 tonne excavator at roof level to determine the lateral capacity and failure mechanisms of the tested elevation.

2 TEST BUILDING DESCRIPTION

The test building, located at 27 Rutland Street in the Auckland CBD, was a relatively prototypical unreinforced clay brick masonry building (Walsh et al. 2014), that was originally constructed in 1931. The building had floor dimensions of approximately 10 m in the E-W direction and 12 m in the N-S direction (see Fig. 1). The building consisted of four storeys – three storeys above grade (approximately 11.3 m from grade to the top of the reinforced concrete (RC) parapet at the north elevation) and a basement level. The primary gravity loadbearing elements of the building consisted of URM piers and walls. A continuous RC bond beam extended around the full perimeter of the building at the roof level, on which timber roof trusses were supported. RC bond beams at all other storey levels extended around the perimeter of the building (excluding the east elevation), where the RC beams acted as window lintels. Steel angle lintels were used over the few small openings on the east URM wall.

The original floor diaphragm construction consisted of timber joists spanning in the N-S direction, sized primarily 280 mm x 50 mm with an average centre-to-centre spacing of 420 mm. A concrete encased Rolled Steel Joist (RSJ) column was positioned at the centre of the building, supporting a concrete encased steel beam spanning in the E-W direction which in turn supported the timber joists at all floor levels (except for the roof level). Tongue and groove timber flooring, with an approximate thickness of 20 mm, was used at all floor levels. The roof of the subject building was supported by three large timber trusses spanning E-W and supporting timber purlins and plank sheathing. The building foundation consisted of shallow RC strip and spread footings supporting URM walls and piers. All interior partitions

walls and any “false floors” that were installed on top of the tongue and grove flooring were removed prior to testing. No interior URM or load-bearing partition walls were present in the building during pushover testing.

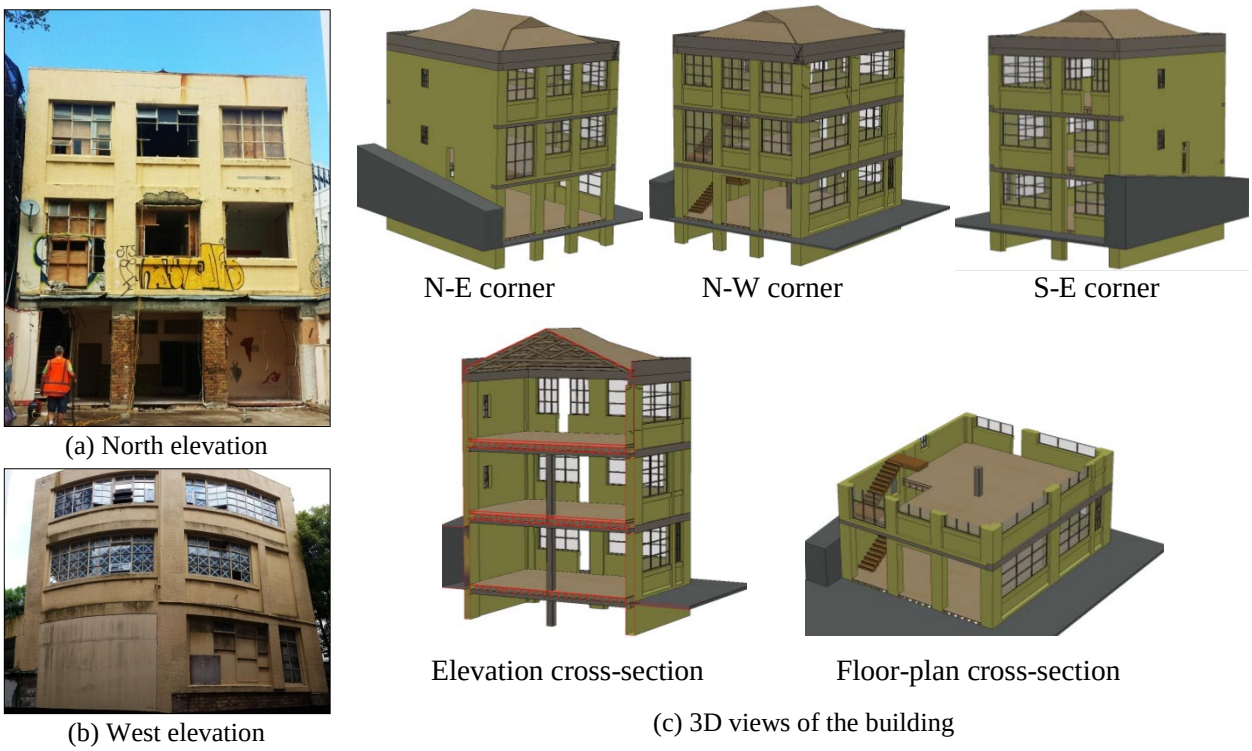

(a) North elevation

(b) West elevation

(c) 3D views of the building

Figure 1. The tested building located at 27 Rutland Street, Auckland CBD

2.1 *Material Properties*

Samples were extracted from the test building to quantify the material properties of the masonry, steel reinforcement, and concrete bond beams. The characteristic strengths for these materials are summarised in Table 1 along with the test standards used in determining these properties.

Table 1. Material characteristics of test building located at 27 Rutland Street

Characteristic	Mean (MPa)	Characteristic	Mean (MPa)
Mortar compression strength, $f_j'^{(1,2)}$	4.3	Masonry prism density, ρ_m (kg/m^3)	1830
Brick compression strength, $f_b'^{(3)}$	20.8	Concrete compressive strength, $f_c'^{(7,8)}$	18.5
Brick modulus of rupture, $f_{br}'^{(3)}$	2.8	Concrete splitting strength, $f_{ct}'^{(9)}$	2.1
Masonry bed joint shear strength, $f_{jv}'^{(4)}$	0.44	10-mm reinf. steel yield strength, $f_{sy}'^{(10)}$	267
Masonry prism compression strength, $f_m'^{(5)}$	6.3	10-mm reinf. steel ult. strength, $f_{su}'^{(10)}$	364
Masonry prism elastic modulus, $E_m^{(5)}$	5630	12.7-mm reinf. steel yield strength, $f_{sy}'^{(10)}$	312
Masonry prism bond strength, $f_{fb}'^{(6)}$	0.34	12.7-mm reinf. steel ult. strength, $f_{su}'^{(10)}$	421

1. ASTM C109/C109M-13 (2013)
2. Lumantarna (2012)
3. ASTM C67-11 (2011)
4. ASTM C1531-09 (2009)
5. ASTM C1314-11a (2011)
6. ASTM C1072-11 (2011)
7. NZS 3112.2 (1986)
8. ASTM C39/C39M-14 (2011)
9. NZS 3112.2 (1986)
10. ASTM A370-12a (2012)

3 TESTING METHODOLOGY

Pushover testing of the subject building was simulated using a 22 tonne excavator (see Fig. 2). The west elevation of the subject building was selected for testing due to accessibility and reduced potential risks to public spaces, as well as the large window openings on the elevation which formed three load resisting URM piers (see Fig. 1 and Fig. 2). Rocking of the URM piers was predicted to occur at the maximum point load expected to be applied by the excavator (NZSEE 2015; Pir et al. 2015).

Control limitations inherent in the adopted loading method restricted the ability to apply a predefined loading protocol to the subject building elevation. Instead, a series of load applications and releases were applied by the excavator to simulate cyclic loading. Eight loading cycles were applied to the structure in total, with point load magnitude ranging between 20 kN and 60 kN. Loading was only applied in the south direction as the excavator was unable to pull the elevation in the north direction.

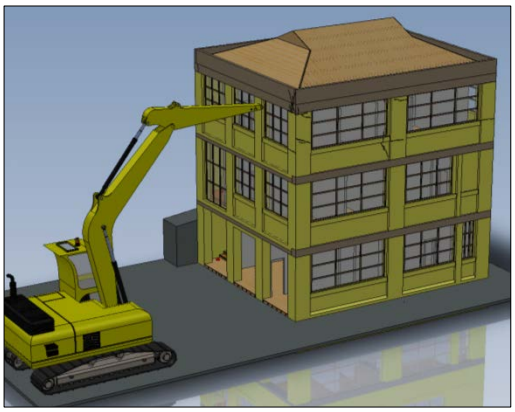

(a) Schematic showing loading of N-W corner

(b) Photograph of north elevation prior to load application

Figure 2. Excavator preparing to apply load for pushover testing

The overall load deformation response was measured with a load cell fixed at the roof level at the point of load application. A larger area steel plate was directly attached to the load cell and was used for the excavator to apply loads to the building without inducing damage to the load cell (see Fig. 3 and Fig. 4d).

(a) Close-up of load application

(b) Maximum load application of the 22 tonne excavator

Figure 3. Loading of the building corner

(a) Interior view of second storey test wall facing west showing instrumentation

(b) Middle pier, close-up of instrumentation

(c) Installation of external instrumentation

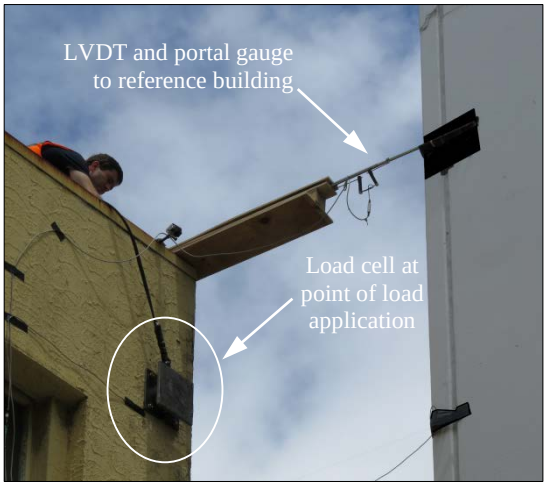

(d) Load cell with loading plate and LVDT to reference building

Figure 4. Test instrumentation

Due to the anticipated rocking mechanism of the second storey piers, insignificant lateral load was expected to be transferred to the lower storey URM piers. In addition, limited site access and tight time restraints resulted in only the second storey URM piers being heavily instrumented (see Fig. 4a). Vertical deformations at the ends of each URM pier were measured to quantify pier uplift and rotation. The components of flexural and shear deformation were determined for the middle URM pier only. The overall displacement of the building near to the point of load application was measured with an exterior LVDT and portal strain gauges mounted to the roof and measuring displacements relative to the adjacent "reference" building (see Fig. 4d).

4 OBSERVED DAMAGE AND BEHAVIOUR

4.1 *Global Behaviour*

Following completion of eight loading testing cycles, horizontal cracking was observed at the top and bottom of each of the second storey URM piers (see Fig. 5). The observed crack pattern was consistent with the predicted rocking response of the second storey URM piers. No cracking was observed on either the first or ground storeys, suggesting that as expected, the pier rocking limited the force transfer to the lower storeys. Multiple cracks radiating away and around the load cell were observed that appeared to be local effects of masonry damage at the point of load application.

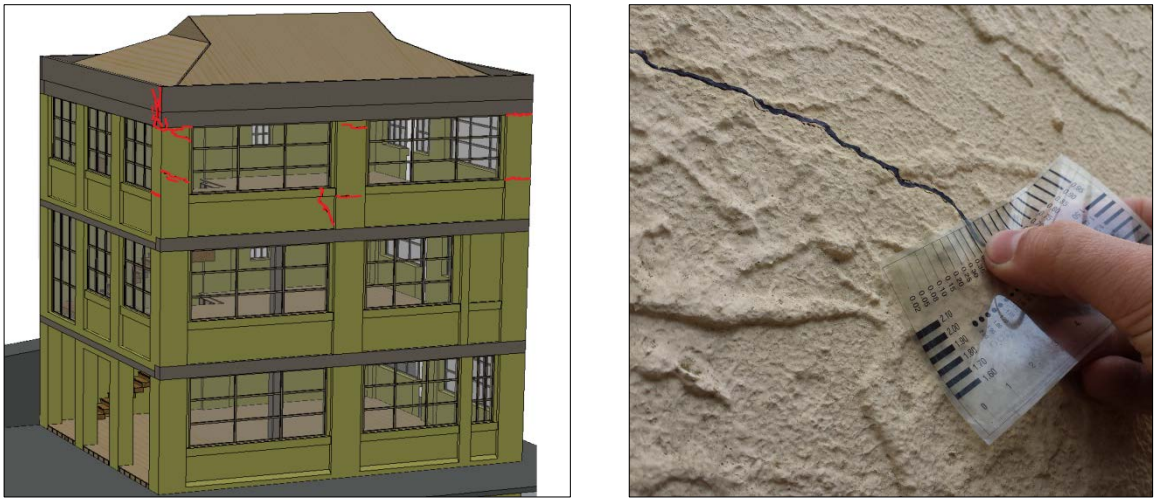

(a) Observed crack damage (marked in red)

(b) Observed cracks ranged from 0.1 mm to 2.0 mm in width

Figure 5. Observed cracking damage

The force-displacement behaviour of the west elevation is shown in Figure 6. Overall the west elevation of the test building behaved in an elastic manner, with a consistent secant stiffness of approximately 16 kN/mm for each cycle. It should be noted that due to data acquisition complications, the initial cracking was not captured and as such the force-displacement response shown in Figure 6 represents the cracked section behaviour for each cycle. The consistent secant stiffness observed is likely to be a result of all cycles representing the cracked section behaviour.

Approximately 1 mm of residual displacement was observed during testing. This small amount of residual displacement may be attributed to the local damage to the masonry in the area surrounding the applied load. The lack of significant residual displacement also suggests that sliding of the concrete bond beam on the top of the masonry piers did not occur and that the URM piers likely re-centred following load release.

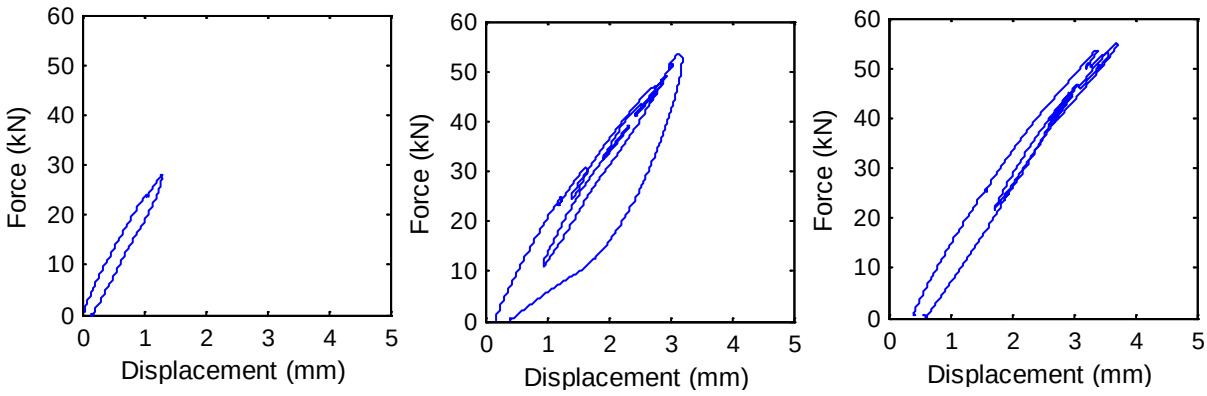

(a) Cycle 1 (b) Cycle 3 (c) Cycle 4

Figure 6. Selected force-displacement cycles of test wall at roof level

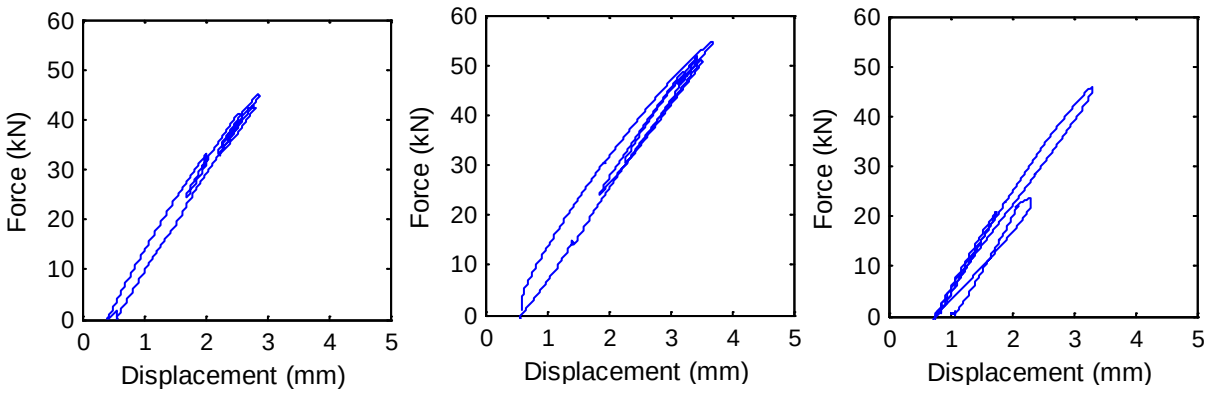

(d) Cycle 5 (e) Cycle 6 (f) Cycle 8

Figure 7. (cont) Selected force-displacement cycles of test wall at roof level

4.2 *Pier Behaviour*

The pier rotations with respect to applied loads are shown in Figure 7 in which both the rotations at the top and bottom of each pier are shown for the uni-directional loading (i.e., no "negative" loading was applied because the excavator could only push the building). Rotations at the top of the piers were approximately four times greater than at the bottom, which is consistent with the large cracks observed at the pier tops after testing, suggesting that flexural deformation occurred in the piers. This flexural deformation contradicts the assumption that during pier rocking, the piers behaved as effectively rigid bodies. However, this flexural deformation likely improved the behaviour of the piers, as the differential rotation at the top and bottom of the piers reduced the overall rotation and overturning moment generated by P-Δ effects. As such, the current assessment practice of assuming the piers to act as rigid bodies is likely conservative at small drift levels.

While the overall rotations for the north and middle piers were similar, the south pier experienced rotations of approximately twice the magnitude of the other piers at cycles with loading above 30 kN (see Fig. 7). This increased rotation was most likely a result of the flange orientation at the north and south piers and the uni-directional loading. Because the load was applied in only one direction, the north and south piers would be expected to have different lateral behaviour as their flanges were mirrors of each other (see Fig. 8). In the south pier, the flange was located on the compression face. When rocking initiated, the in-plane portion of the south pier cracked and the flange resisted the compression force. Because the flange was rocking out-of-plane, the moment of inertia resisting the lateral load in the south pier was smaller than in the other two piers. Additionally, the weight of the flange and the roof load acted on the compression side of the neutral axis, thereby providing additional overturning moment and increasing the south pier rotation. Conversely, the north pier flange was located on the tension side of the section (see Fig. 8). When cracking initiated through the flange, the north pier still had the majority of the in-plane portion to resist load, which had a much larger moment of inertia than the cracked section of the south pier. Also, the self-weight and roof load were located such that they acted to resist overturning and as a result worked in to supplement the larger moment of inertia of the north pier to reduce the overall rotations.

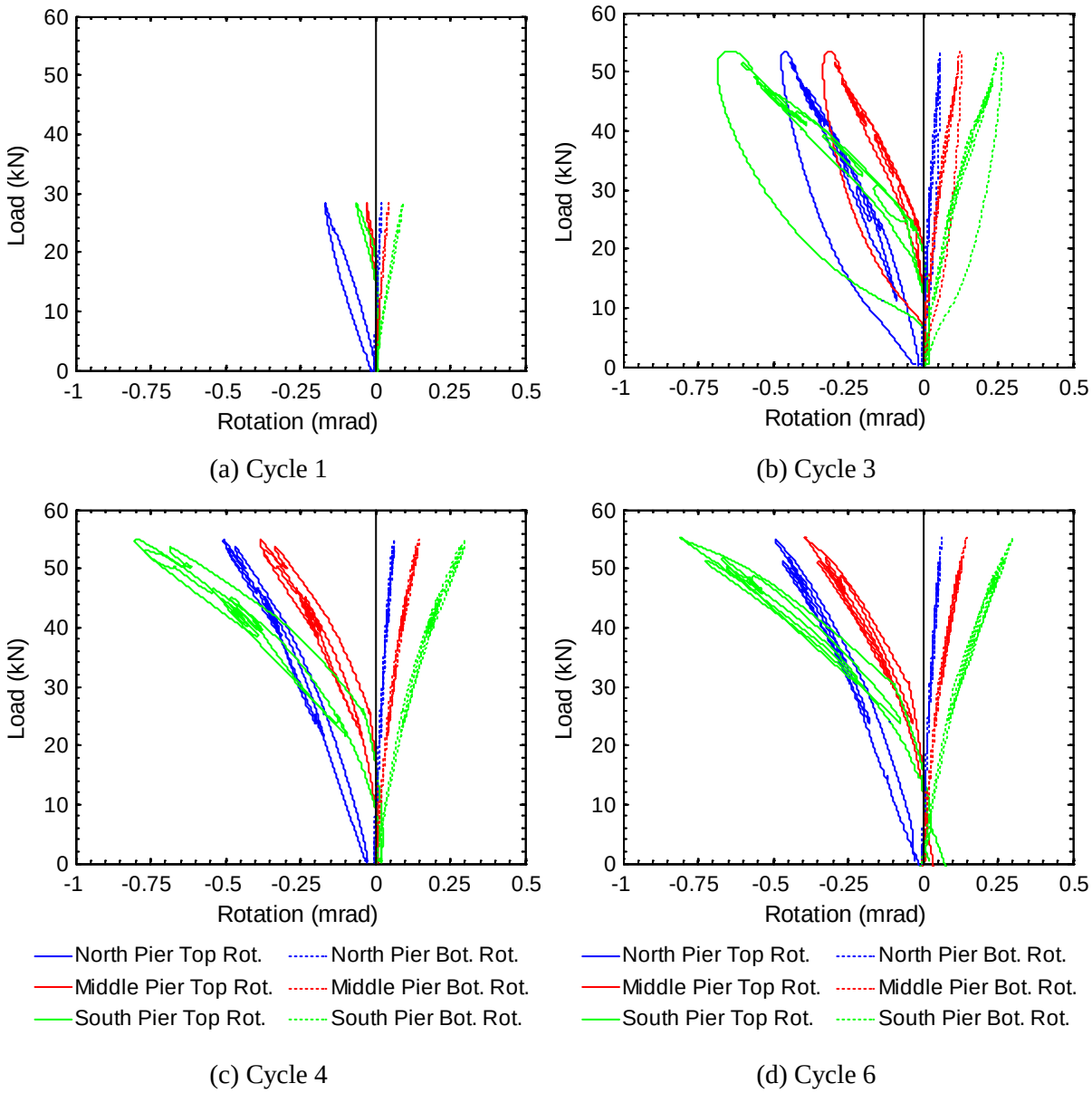

(a) Cycle 1 (b) Cycle 3

(c) Cycle 4 (d) Cycle 6

Figure 8. Selected pier rotation cycles of test building at the second storey

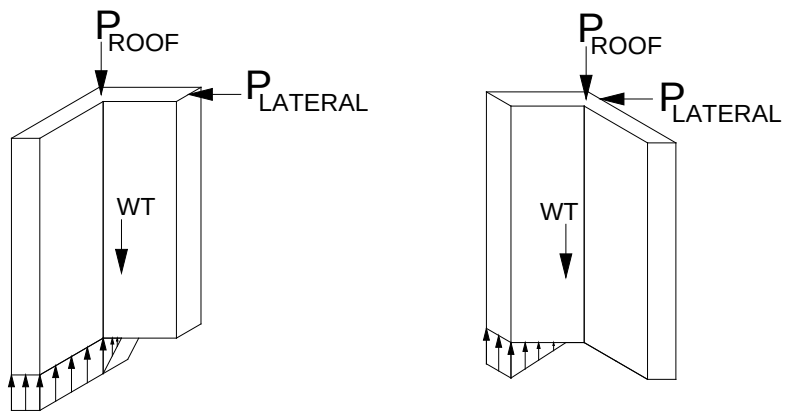

(a) Load distribution on South Pier (b) Load distribution on North Pier

Figure 9. Corner pier load distribution

The relative contributions of the different deformation mechanisms that formed in the middle pier during loading are charted in Figure 9 in order of increasing drift, neglecting discrete cycles and simulating a monotonic push-over loading protocol. Note that the relative contribution from flexure reduced significantly at higher drift demands as was expected, and rocking appears to have gradually increased in relative contribution as drift demands increased. The contribution to total panel deformation from rocking was determined to have a positive correlation with increasing load (particularly with the impulse loads occasionally applied during testing; hence the "spikes" in rocking contribution at various locations in Fig. 9), and the contribution to total panel deformation from shear was found to have a negative correlation with increasing load. Hence, any residual deformations in the pier (however small) were due mostly to shear deformation.

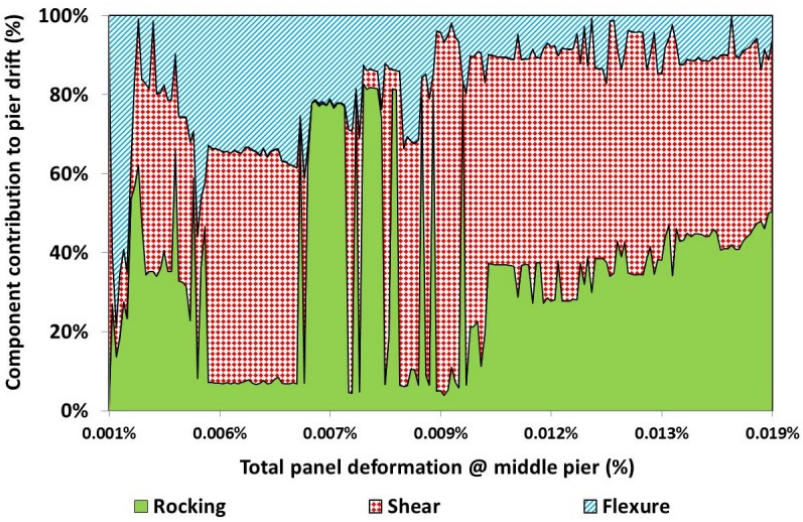

Figure 10. Relative contributions from deformation mechanisms of the middle pier at the second storey

5 CONCLUSIONS

A full-scale pushover testing of an existing vintage URM building was successfully performed in order to provide valuable inputs for the development of seismic assessment tools. The observed crack pattern was consistent with the predicted rocking response of the second storey URM piers of the subject building. No cracking was observed on either the first or ground storeys, suggesting that as expected, the pier rocking limited the force transfer to the lower storeys. The RC bond beams seem to provide adequate load transfer for load distribution among URM piers, and no sliding was suspected during loading. From the testing it was observed that the overall the west elevation of the test building behaved in an essentially elastic manner, with a consistent secant stiffness of approximately 16 kN/mm for each cycle. Rotations at the top of the URM piers were approximately four times greater than at the bottom, this flexural deformation contradicts the assumption that the piers behaved as effectively rigid bodies during pier rocking. However, this flexural response reduces with increased drift and it is likely that at larger drifts the rocking response will come to dominate the pier behaviour.

6 ACKNOWLEDGEMENTS

The authors are grateful for the in-kind donations provided by DND Development Ltd. (owners of the building), Peter Ward of Ward Group (demolition contractor in charge of the site), Racquel Lewis of Titivate Ltd, and Luke Austin of LADRA. Megan McNichols, Serguei Khairov, Yuri Dizur, Jerome Quenneville, Ronald Gultom, Marat Khassenov, Laura Putri, and Royce Chin assisted with documenting building geometry and mobilising test equipment. Royce Chin, Mark Byrami, and Ross Reichardt assisted with materials testing. EQ STRUC Group is thanked for supplying equipment and on-site assistance.

7 REFERENCES

ASTM International. ASTM A370-12a: Standard Test Methods and Definitions for Mechanical Testing of Steel Products. West Conshohocken, Pennsylvania; 2012. doi: 10.1520/A0370-12A.

ASTM International. ASTM C39/C39M-14: Standard Test Method for Compressive Strength of Cylindrical Concrete Specimens. West Conshohocken, Pennsylvania; 2011. doi: 10.1520/C0039_C0039M-14A.

ASTM International. ASTM C67-11: Standard Test Methods for Sampling and Testing Brick and Structural Clay Tile. West Conshohocken, Pennsylvania; 2011. DOI: 10.1520/C0067-11.

ASTM International. ASTM C109/C109M-13: Standard Test Method for Compressive Strength of Hydraulic Cement Mortars (Using 2-in. or [50-mm] Cube Specimens). West Conshohocken, Pennsylvania; 2013. doi: 10.1520/C0109_C0109M-13.

ASTM International. ASTM C1072-11: Standard Test Methods for Measurement of Masonry Flexural Bond Strength. West Conshohocken, Pennsylvania; 2011. DOI: 10.1520/C1072-11.

ASTM International. ASTM C1314-11a: Standard Test Method for Compressive Strength of Masonry Prisms. West Conshohocken, Pennsylvania; 2011. DOI: 10.1520/C1314-11A.

ASTM International. ASTM C1531-09: Standard Test Methods for In Situ Measurement of Masonry Mortar Joint Shear Strength Index. West Conshohocken, Pennsylvania; 2009. DOI: 10.1520/ C1531-09.

Knox, C. Assessment of perforated unreinforced masonry walls responding in-plane. Doctoral Dissertation, The University of Auckland, Auckland, New Zealand; 2012.

Lumantarna, R. Material Characterisation of New Zealand's Clay Brick Unreinforced Masonry Buildings. Doctoral Dissertation, The University of Auckland, Auckland, New Zealand; 2012.

NZSEE (New Zealand Society for Earthquake Engineering). Assessment and Improvement of the Structural Performance of Buildings in Earthquakes, Recommendations of a NZSEE Project Technical Group. Incorporated Corrigenda No. 4, Section 10, Seismic Assessment of Unreinforced Masonry Buildings, New Zealand Society for Earthquake Engineering, Wellington, New Zealand; 2015.

Pir, A., Hogan, L., Dizhur, D., Walsh, K., Ingham, J. A Comparison of Numerically and Experimentally Obtained In-Plane Responses of a Full-Scale Unreinforced Masonry Wall. 10th Pacific Conference on Earthquake Engineering, Sydney, Australia, November 6 – 8, 2015.

Standards New Zealand (NZS). NZS 3112.2 Part 2: Tests Relating to the Determination of Strength of Concrete. Wellington, New Zealand; 1986.

Walsh, K. Q., Dizhur, D. Y., Lmesfer, N., Cummuskey, P. A., Cousins, J., Derakhshan, H., Griffith, M. C., Ingham, J. M. 2014. Geometric characterisation and out-of-plane seismic stability of low-rise unreinforced brick masonry buildings in Auckland, New Zealand. *Bulletin of the New Zealand Society for Earthquake Engineering*. 47 (2): 139-156